Journal of Engineering Sciences
Vol 10, Issue 11, Nov /2019
ISSN NO:0377-9254

POWER SYSTEM COMPENSATION USING CUSTOM POWER ACTIVE TRANSFORMERS

L.Vinod Kumar*, B.Neelimadevi**
*,**Dept. of Electrical and Electronics Engineering, Nalanda Institute of Engineering and Technology, Sattenapalli - 522438. AP, India.

Email: vinodkumarloya@gmail.com

ABSTRACT- With the global trend to produce clean electrical energy, the penetration of renewable energy sources in existing electricity infrastructure is expected to increase significantly within the next few years. The custom power active transformer (CPAT) is expected to play essential role in future smart grid topologies. Thus, it provides power system services using a single transformer. The CPAT equipped with a power converter can be utilized in distribution systems to control grid current and load voltage waveforms while operating as a step-up or step-down transformer between the grid and load. Moreover, it can provide other services that any typical shunt-series compensation arrangement provides. The design and analysis of a single-phase CPAT are presented, showing the effect of coupling between windings and transformer parameters affecting CPAT operation. In this project, control of the CPAT in a unified power-quality controller application is investigated to attenuate grid-current and load-voltage harmonics as well as compensate for reactive power requirements and mitigate grid inrush current. The proposed power electronic transformer has been modeled by using MATLAB/ SIMULINK and Power quality improvement with proposed model has been verified by the simulation results.

I. INTRODUCTION

Surveying the recent history of electrical power systems and the electrical industry reveals the rapidly increasing concern of power quality, and this term is becoming clearer and more important for both end users and electrical utilities stakeholders in terms of electricity generation, transmission and distribution. The issues of the power quality, such as voltage levels and reactive power transmission, have many different solutions, which make optimum choices for the best quality complex, often necessitating creative combinations of several techniques by engineers. It is necessary to identify the problem type and characteristics in order to devise optimal solutions that provide power quality with cost efficiency, minimizing the massive investment required for power infrastructure and maintenance. Power Electronic (PE) intervention has several forms and impacts on the electrical network, especially in the transmission networks, wherein this technology has proved its efficiency in HVDC transmission, and studies are in progress to use it in other parts of the electrical network from generation down to LV distribution networks. However, there are several technical and business factors that need to be considered before applying PE approaches in novel areas of the network, such as making it commonplace in distribution networks.

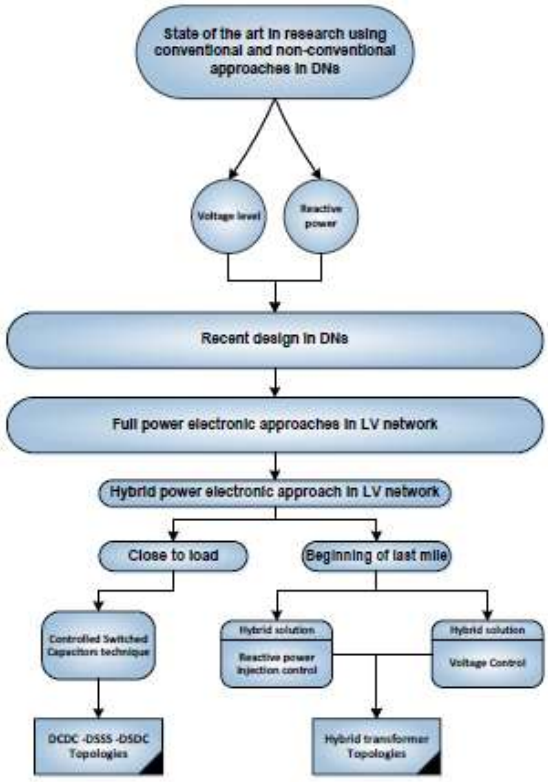

Fig.1: Thesis layout.

Therefore, more efforts are needed to prove that the cost and losses of deploying PE designs can be ignored comparison to the technical and long-term benefits, Also more characterization is needed for novel designs that can meet the current and future network challenges with less losses and costs.This study evaluates recent research and designs for the proper area regarding deploying PE in electrical networks in order to meet the challenges at that area that their solutions not carried out practically in the network. The introduced approach takes into consideration the losses and high costs that were introduced by several designs and approaches that meet various challenges currently and in future. The layout of the reached contribution to knowledge is shown in the following figure 1 for illustration.

Journal of Engineering Sciences
Vol 10, Issue 11, Nov /2019
ISSN NO:0377-9254

II. SYSTEM MODELING

Based on magnetic circuits theory, windings wound over a common core are equivalent to shunt electrical circuits while windings wound over shunt cores are equivalent to series electrical circuits. The construction of a single-phase transformer with auxiliary windings that are equivalent to shunt and series circuits is presented in Fig. 2 which forms the basic concept of a single-phase CPAT. The configuration in Fig. 2 shows the structure of a single-phase CPAT with primary voltage vprim, secondary voltage vsec, shunt compensation current ishand series compensation voltage vser. In order to realize the theory of operation of the CPAT, an equivalent magnetic model of the structure is derived through the conventional modeling approach of magnetic circuits using electric circuit analogy. However, the accuracy of the magnetic circuit is related to the assumptions made to transform the magnetic core into an equivalent magnetic circuit. Transformation of this magnetic structure to a magnetic circuit requires identification of magnetic paths to be represented by reluctances. The equivalent magnetic circuit in Fig. 3(a) represents the transformer in Fig. 2 with F as the induced magneto-motive force (mmf) from each winding, Φ as the flux in each limb and R as the equivalent magnetic reluctance in the transformer core and air. Subscripts prim, sh, serand sec represent parameters of primary, shunt, series and secondary windings, respectively. Due to the existence of non-linear characteristics in the iron core, a non-linear reactance is used to represent each iron limb and a linear reactance for leakage air path. Non-linear reluctances RY and RL represent yoke and limb iron core modelled as an opposing mmf source following the B-H characteristics of the core material. Meanwhile, winding leakage reluctances Rlprim, Rlsec, Rlsh,Rlser and core leakage reluctance R0 are linear reluctances representing leakage flux through air. These reluctances are calculated based on limb length and cross-sectional area.The magnetic circuit is affected by the applied voltage and currents in the winding electric circuit shown in Fig. 3(b). Each mmf source in Fig. 3(a) is coupled to a winding electric circuit in Fig. 3(b) consisting of winding resistance (Rw) and core losses equivalent resistance (Rc). However, with a non-ideal transformer, the difference between primary and secondary voltage harmonics combined with the non-linearity of core reluctances (RL ,RY), can introduce extra components in the current as shown. Nevertheless, this effect can be considered minimal based on design consideration of the core. Moreover, these effects can be attenuated through the shunt winding as well when accompanied by an appropriate controller.

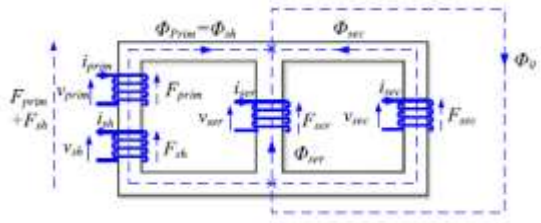

Fig.2: Configuration of a single-phase CPAT.

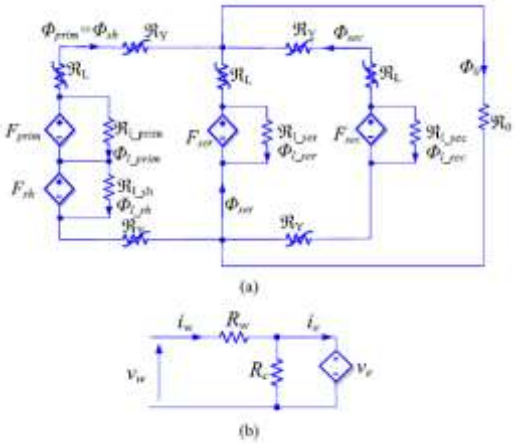

Fig.3: Equivalent model of a single-phase CPAT (a) equivalent magnetic circuit and (b) winding and core-losses electric circuit.

Considering flux is mainly affected by the voltage, harmonic voltages from the primary can be attenuated at the secondary through the applied voltage on the series winding. This performance is mainly affected by the core leakage reluctance (R0), a decrease in R0 would amplify the effect of RL which is nonlinear and would add up harmonic components on the secondary flux. However, R0 is typically low and with design considerations, core leakage can be minimized to achieve the required performance. The presence of an equivalent shunt and series circuit from the configuration in Fig. 2 can be observed by transforming the magnetic circuit in Fig. 3 to a topologically correct equivalent electric circuit model through the principle of duality discussed. The duality equivalent circuit shown in Fig. 4 is represented by the elements L as the equivalent inductance of each reluctance. It can be observed that vsh is equivalent to a shunt circuit to the primary winding while vser is equivalent to a series circuit between the primary and secondary.

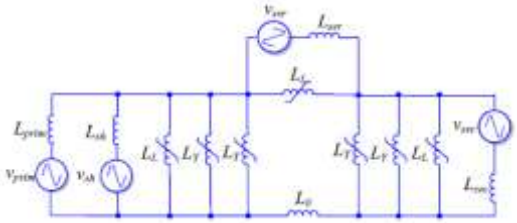

Fig.4: Equivalent electric circuit of a single-phase CPAT.

Extension of the single-phase CPAT to three-phase applications could be achieved by using three-single-phase CPATs where each CPAT represents a single-phase with series and shunt compensation. This is a suitable configuration when the three-phase CPAT is compared to a three-phase compensation system consisting of multiple single-phase transformers. Another approach is to stack all the three CPAT cores on top of each other as in a typical three-phase shell type transformer. The resulting structure would share common yokes between phases as well as reduce required number of tanks, bushings, protection equipment and footprint.The main characteristics of CPAT

as compared to the conventional multi-transformer approach (series and shunt compensators connected to the grid using separate insolation transformers with a distribution transformer in between) can be summarized into size reduction and facilitating services to the grid. In a multi-transformer approach, two windings per phase and per transformer are required. Therefore, the total number of windings required in a single-phase system would be 6 p where p is the number of phases. The CPAT requires 4 p windings to achieve the same objective. Assuming the number of turns are identical, this yields a total number of windings reduction of 33%.Meanwhile, size of the resulting CPAT structure combines the three single-phase core type transformers into one, replacing two transformers with one central limb in the main transformer. The CPAT enables utilization of a single transformer with controlled flux to provide services to the load, transformer and grid such as reduced inrush currents, harmonics elimination, voltage regulation, reactive power compensation and other grid supportive services based on the control technique. As compared to the multi-transformer approach, the CPAT eliminates the requirement of high voltage/current handling windings usually present in the grid side of series and shunt isolation transformers that connects power electronic converters to the system. The overall reduction in cost and the integration of power converter with transformer as a single unit makes it an attractive approach to minimize the requirement of several cascaded compensation systems.In a distribution system, the single phase CPAT in Fig. 2 can be combined with a three-phase converter adopted from for UPQC application purposes as shown in Fig. 5. The objective of the shunt winding in the proposed UPQC is to achieve sinusoidal grid current, damp grid current during transients, compensate for reactive power requirements and maintain a constant DC bus voltage. The series winding would be required to achieve sinusoidal load voltage and regulate load voltage magnitude. In Fig. 5, leg ‘a’ of the converter is connected to the series winding through an LC filter where the voltage across the capacitor is controlled in order to achieve the required series compensation voltage. Leg ‘b’ of the converter is connected to the shunt winding through an LCL filter where the filter output current iscontrolled according to the required shunt compensation. Design of the series filter inductor (La), shunt filter inductors (Lb1 and Lb2), series capacitor (Ca) and shunt capacitor (Cb) are based on the required control bandwidth and the switching frequency of the converter. Passive damping of the LC and LCL resonance is accomplished through damping resistance Ra and Rb.

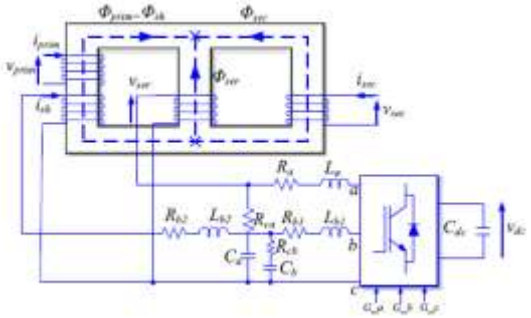

Fig.5: Configuration of single-phase CPAT for UPQC application.

Leg ‘c’ is the common leg between both windings and represents the current return path of both phases. Having a common leg for both compensation presents a control challenge due to coupling between the converter legs. Among the strategies proposed in the literature to decouple the control of each leg, the strategy in based on Three-Leg UPQC Space Vector Modulation (TL-UPQC SVM) is utilized due to its simplicity and effectiveness. The resulting gate signals G a ,G b and G c are used to control the converter switches. Assuming a non-linear load connected at the secondary winding of the transformer, harmonic currents on the secondary winding arise. Since the secondary limb magnetic circuit is in parallel to the primary limb, both primary winding and shunt winding would handle a similar mmf waveform. Injection of shunt compensation current adjusts the required mmf from the primary and hence changing the required primary current. With such an approach, harmonic components present in isec can be compensated by ishsuch that the resulting iprim is harmonics free. Moreover, ishwould be absorbing fundamental frequency current to charge DC bus vdc, compensating the reactive power required by the primary winding and reducing the transient current required from the grid. Considering vprim consists of harmonic components, they can be attenuated from arriving at the secondary winding by varying vser such that the resulting Φsec is sinusoidal and therefore the vsec would be sinusoidal too. Moreover, the magnitude of the fundamental frequency of vsec can be controlled by injecting the fundamental component in vser to compensate for voltage swells and sags from the primary.

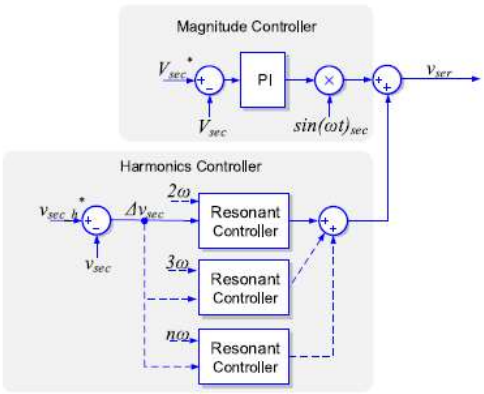

Fig.6: Series compensation control loop of single-phase CPAT-UPQC.

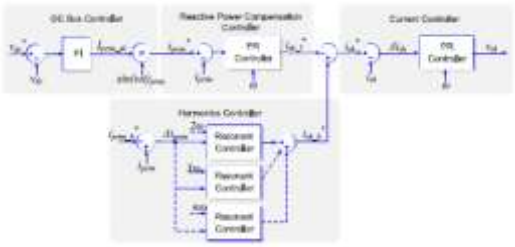

Fig.7: Shunt compensation control loop for single-phase CPAT-UPQC.

The control architecture presented in Figs. 6 and 7 consists of two part controllers; shunt and series

compensation. Series compensation shown in Fig. 6 consists of two parts; magnitude of the secondary voltage Vsec is maintained constant at the reference value Vsec through a PI controller. The resulting command voltage is multiplied by the secondary voltage synchronizing signal sin(ωt)sec in order to achieve an in-phase compensation of the secondary voltage magnitude. Meanwhile secondary voltage harmonics are compensated through Resonant (R) controllers tuned to required compensating frequencies nωwhere n represents the harmonic order and a reference secondary voltage harmonics vsec h set to zero. Resonant controllers are utilized due to their high gain at selected frequencies and no phase shift or gain at other frequencies. Therefore, the controller would generate a command voltage at the selected frequency which would attenuate the error. The resulting sum of command voltages from the PI and R controllers obtains the required injected voltage vser, which is the output voltage from leg 'a' with respect to leg 'c' in the single-phase setup in Fig. 5. The shunt compensation controller in Fig. 7 consists of four controllers; two controllers control the fundamental component of primary current, one is used for compensation of harmonic components and a shunt winding current controller which achieves the required reference current from the previous controllers. The DC bus voltage controller maintains a constant reference voltage vdc across the converter capacitor by absorbing active power from the primary winding of the transformer. The PI controller determines the required capacitor charging current Iprim dc. Iprim dc is synchronized with the fundamental primary voltage sin(ωt)prim to acquire the reference primary current iprim. iprim and feedback primary current iprim are passed on to a (Proportional Resonant) PR controller tuned at the fundamental frequency in order to obtain the required fundamental shunt compensation current ishf. The reference current would maintain a constant DC bus voltage, zero-reactive power from the primary winding and would dampen the primary current during transients. Primary harmonic currents are compensated through R controllers with a reference iprimh which is set to zero. This obtains the required shunt compensation harmonic currents ishh. The combined compensation current ishis controlled through a PR controller to obtain the required converter shunt output voltage vsh. Primary frequency ω, synchronizing signal sin(ωt)prim, secondary voltage magnitude Vsec and secondary voltage synchronizing signal sin(ωt)sec are obtained through a Double Second-Order Generalized Integrator Frequency Locked Loop (DSOGI-FLL).

III. SIMULATION RESULTS

To investigate the effectiveness of series harmonic compensation, the primary voltage was generated through a combination of harmonic components 3rd, 5th, 7th and 9th with the proportions 25%,12.5%, 6.25% and 3.13% of fundamental component respectively. Shunt harmonics compensation was investigated by connecting a non-linear load at the terminals of the secondary winding to withdraw non-linear, active and reactive current with the harmonic spectrum consisting of 3rd, 5th, 7th and 9th with the proportions 23%, 6.34%, 1.56% and 0.85% of fundamental component respectively. Meanwhile, secondary voltage magnitude control was examined by applying voltage disruption during operation. Primary current transient damping was investigated by suddenly applying voltage to the primary winding to observe the inrush current effect with and without compensation.

A. HARMONICS ATTENUATION, VOLTAGE REGULATION AND REACTIVE POWER COMPENSATION

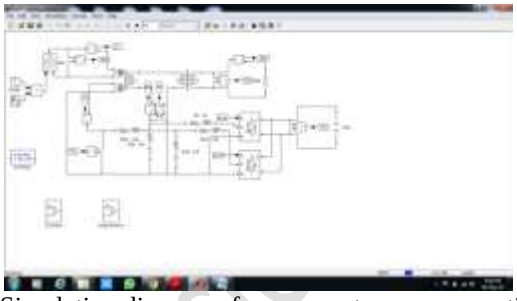

Fig:8. Simulation diagram of power system compensation.

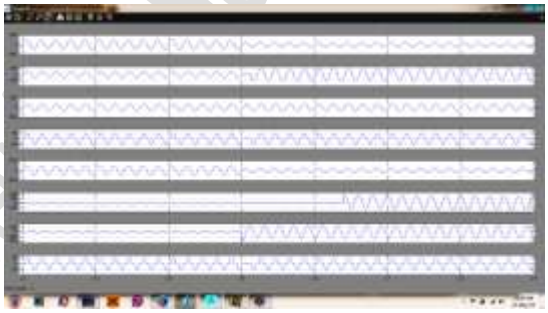

Fig:9. Voltage and current waveforms during 50% primary voltage sag.

During a primary voltage sag of 50% illustrated in Fig. 9, the secondary voltage magnitude controller increases the fundamental frequency component of the injected series voltage *v*ser to compensate for this drop. It should be noted that the secondary voltage harmonic contents changes as the transformer is loaded.

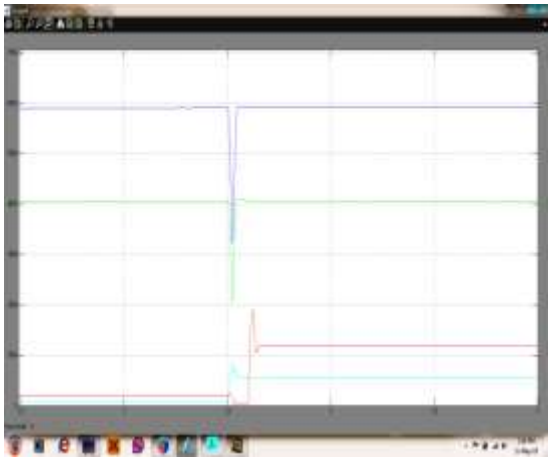

Fig:10. Active Power variation during a 50% primary voltage sag.

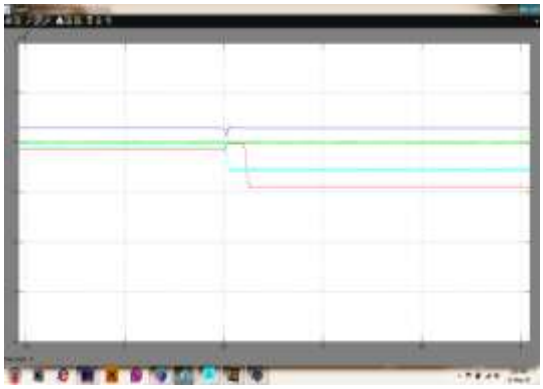

Fig:11. Reactive Power variation during a 50% primary voltage sag.

This is typically due to the inductive action of the transformer under load acting as a filter reducing the harmonic contents of the secondary voltage. However, this yields a voltage drop to the load voltage and the presence of magnitude controller is essential. Based on the transformer design, such drop can be minimized by considering low core leakage impedance which yields a higher reluctance path of yokes and end limbs as discussed. The effect of the sag can be observed on the power exchanged between the converter and the grid in Fig. 10 and Fig. 11.

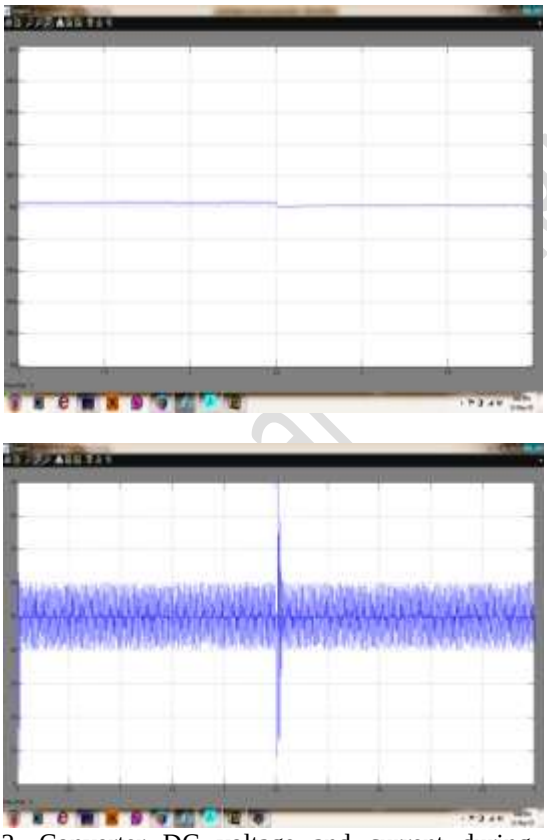

Fig:12. Converter DC voltage and current during 50% primary voltage sag.

The shunt leg of the converter absorbs more active power to supply the series leg to supply the difference in the voltage. This can be also be observed in the DC bus voltage and current in Fig.12.

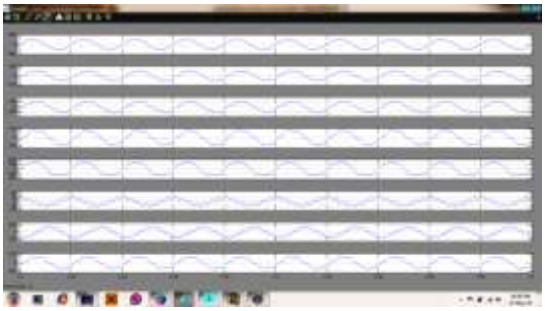

Fig:13. Voltage and current waveforms with shunt harmonics compensation.

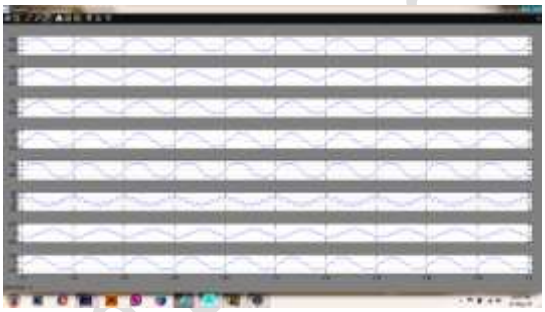

Fig:14. Voltage and current waveforms with series harmonic compensation.

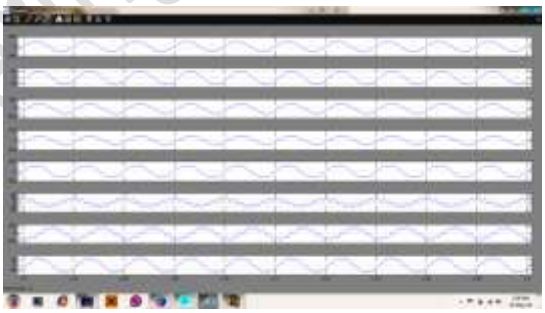

Fig.15. Voltage and current waveforms with reactive power compensation.

As the series leg demands more power, the DC bus voltage decreases until the shunt controller provides sufficient power to the DC bus. Enabling the shunt harmonics controller results in the injected current shown in Fig. 13 which includes harmonic components required by the load. The series harmonics controller injects harmonic voltages into the series winding as illustrated in Fig. 14 to attenuate the secondary voltage harmonics. The resulting harmonic components present in the primary current were reduced to 0.05% and secondary voltage to 0.5% which shows the effectiveness of the CPAT in harmonics attenuation. It should be noted that the series harmonics compensator not only compensates for harmonic voltages present in the primary, but also harmonic voltages induced due to the non-linear current absorbed by the load and passing through the transformer equivalent reluctance. Controller parameters and filters affect the bandwidth over which compensation is possible. Moreover, inverter output voltage and current harmonics will affect the resulting compensation. Enabling the reactive power compensator, shunt reactive current was injected into the transformer eliminating the requirement of reactive power from the primary side as shown in figure 15. The required reactive

power by the transformer is dependent on the transformer design and equivalent impedance.

B. INRUSH CURRENT MITIGATION

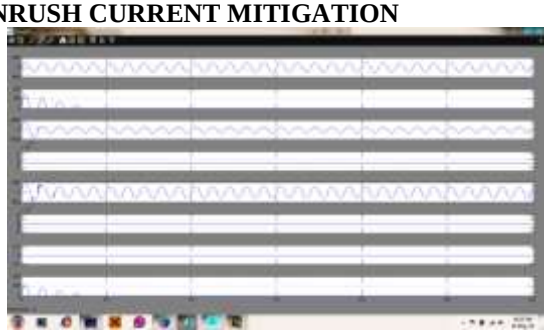

Fig:16. Voltage and current waveforms during inrush transient without compensation.

The reactive power compensation controller can achieve damping of primary current during transients. Therefore, during transformer excitation, the required inrush current can be supplied through the shunt winding to the transformer and thus reducing its impact on the source grid. To simulate inrush current, effect of saturation was taken into consideration in the transformer model as with each limb reluctance represented by a controlled mmf source opposing flux direction based on BH curve characteristics. The inrush current through the transformer when rated primary voltage was applied with no load is shown in Fig.16. The magnitude, harmonics and decay time of the primary current shows the significant impact of the inrush current on the grid. Enabling shunt compensation controllers would dampen the primary current magnitude during such transient. This is achieved through its reactive power compensation controller, which acts directly on the primary current magnitude at fundamental frequency. The reference primary current at startup is zero, since the DC bus is fully charged and thus the reactive power compensation controller would maintain a zero primary current at energization.

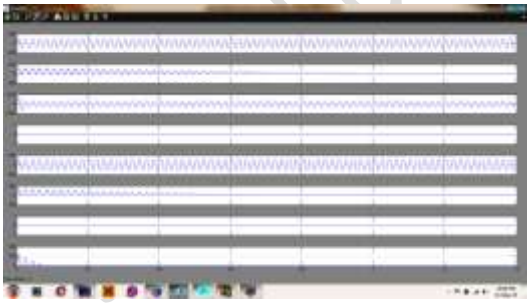

Fig:17. Voltage and current waveforms during inrush transient with compensation.

Moreover, primary current harmonics are mitigated through the primary current harmonics controller. This can be observed in Fig. 17 where the primary current magnitude and harmonics are significantly minimized. However, the transformer still absorbs the same inrush current to energize through the primary and shunt windings. Due to the high current passing through shunt winding in this compensation strategy, it should be noted that the simulation presented here is based on operating the converter at extreme conditions where current and applied voltage to the filter are operating beyond nominal rated values and below absolute maximum values. Moreover, the series winding may be shorted at start-up to avoid connection of the filter circuit to the series winding acting as a load. During this operation, DC bus control is disabled to avoid absorbing charging current at start-up through the shunt winding yielding a higher inrush current. Thus, this operation requires a pre-charged DC bus. Another issue which is not addressed in the presented controller is the decaying dc offset, as the inrush current tends to a steady-state.

IV. CONCLUSION

The Custom Power Active Transformer proposed in this project has shown the ability to combine the possibility of series and shunt services in a single transformer. MATLAB/Simulink Simulation results of a single-phase CPAT-UPQC show the ability of the transformer to achieve compensation of primary current harmonics, reactive power, secondary voltage harmonics and secondary voltage magnitude. Moreover, shunt compensation achieved inrush current mitigation during energization of the transformer, reducing the effect of inrush current on the source grid.

REFERENCES

[1] D. Volk, *Electricity Networks: Infrastructure and Operations* (Insights Series), International Energy Agency, Paris, France, 2013.

[2] Ch. Rami Reddy, and K. Harinadha Reddy. "A New Passive Islanding Detection Technique for Integrated Distributed Generation System Using Rate of Change of Regulator Voltage Over Reactive Power at Balanced Islanding." *Journal of Electrical Engineering & Technology* 14.2 (2019): 527-534.

[3] J. D. Van Wyk and F. C. Lee, “On a Future for Power Electronics,” *IEEE Trans. Emerg. Sel. Topics Power Electron.*, vol. 1, no. 2, pp. 59–72, Jun. 2013.

[4] Ch. Rami Reddy and K. Harinadha Reddy “Passive Islanding Detection Technique for Integrated Distributed Generation at Zero Power Balanced Islanding”, *International Journal of Integrated Engineering, 11(6): September 2019.*

[5] Ch. Rami Reddy and K. Harinadha Reddy. "Islanding detection for inverter based distributed generation with Low frequency current harmonic injection through Q controller and ROCOF analysis." *Journal of Electrical Systems* 14.2 (2018).

[6] J. V. Milanovic and Y. Zhang, “Modeling of FACTS devices for voltage sag mitigation studies in large power systems,” *IEEE Trans. Power Del.*, vol. 25, no. 4, pp. 3044–3052, Oct. 2010.

[7] M. Morati, D. Girod, F. Terrien, V. Peron, P. Poure, and S. Saadate, “Industrial 100-MVA EAF voltage flicker mitigation using VSC-Based STATCOMwith improved performance,” *IEEE Trans. Power Del.*, vol. 31, no. 6, pp. 2494–2501, Dec. 2016.

[8] Ch. Rami Reddy and K. Harinadha Reddy. "An efficient passive islanding detection method for integrated DG system with zero NDZ." *International*

Journal of Renewable Energy Research 8.4 (2018): 1994-2002.

[9] F. Z. Peng, Y. Liu, S. Yang, S. Zhang, D. Gunasekaran, and U. Karki, "Transformer-Less unified power-flow controller using the cascade multilevel inverter," *IEEE Trans. Power Electron.*, vol. 31, no. 8, pp. 5461–5472, Aug. 2016.

[10] Y.-S. Lee, L.-P. Wong, and D. K. W. Cheng, "Simulation and design of integrated magnetics for power converters," *IEEE Trans. Magn.*, vol. 39, no. 2, pp. 1008–1018, Mar. 2003.

[11] Ch. Rami Reddy, and K. Harinadha Reddy. "A passive islanding detection method for neutral point clamped multilevel inverter based distributed generation using rate of change of frequency analysis." *International Journal of Electrical and Computer Engineering* 8.4 (2018): 1967.

[12] C. Liang *et al.*, "Harmonic elimination using parallel delta-connected filtering windings for converter transformers in HVDC systems," *IEEETrans. Power Del.*, vol. 32, no. 2, pp. 933–941, Apr. 2017.

[13] M. Tian, J. Yin, and Y. Liu, "Magnetic integration technology in controllable reactor of transformer type constituted by various magnetic materials," *IEEE Trans. Appl. Supercond.*, vol. 24, no. 5, pp. 1–5, Oct. 2014.

[14] Ch. Rami Reddy, and K. Harinadha Reddy. "Islanding Detection Techniques for Grid Integrated DG–A Review." *International Journal of Renewable Energy Research* 9.2 (2019): 960-977.

[15] D. Li, Q. Chen, Z. Jia, and C. Zhang, "A high-power active filtering system with fundamental magnetic flux compensation," *IEEE Trans. Power Del.*, vol. 21, no. 2, pp. 823–830, Apr. 2006.

[16] Reddy, KV Siva, et al. "Resonance Propagation and Elimination in Integrated and Islanded Micro grids." *International Journal of Power Electronics and Drive Systems* 9.3 (2018): 1445.

[17] C. Wang, X. Yin, Z. Zhang, and M. Wen, "A novel compensation technology of static synchronous compensator integrated with distribution transformer," *IEEE Trans. Power Del.*, vol. 28, no. 2, pp. 1032–1039, Apr. 2013.

[18] Suresh, K., et al. "A passive islanding detection method for hybrid distributed generation system under balanced islanding." *Indonesian Journal of Electrical Engineering and Computer Science* 14.1 (2019): 9-19.

[19] Syed, Raheema, et al. "Unit commitment based reliability analysis with contingency constraint." *Indonesian Journal of Electrical Engineering and Computer Science* 16.1 (2019): 74-81.

[20] Ch. Rami Reddy, K. Harinadha Reddy, and K. Venkata Siva Reddy. "Recognition of islanding data for multiple distributed generation systems with ROCOF shore up analysis." *Smart Intelligent Computing and Applications*. Springer, Singapore, 2019. 547-558.